LAWRENCE
LIVERMORE
NATIONAL
LABORATORY

Sensitivity of Global Modeling Initiative CTM predictions of Antarctic ozone recovery to GCM and DAS generated meteorological fields

Daniel Bergmann, Doug Rotman

December 22, 2003

Disclaimer

Sensitivity of Global Modeling Initiative CTM predictions of Antarctic ozone recovery to GCM and DAS generated meteorological fields

David B. Considine
NASA Langley Research Center, Hampton, Virginia

Peter S. Connell, Daniel J. Bergmann, and Douglas A. Rotman
Lawrence Livermore National Laboratory

Susan E. Strahan
University of Maryland, Baltimore County, Baltimore, Maryland

Abstract. We use the Global Modeling Initiative chemistry and transport model to simulate the evolution of stratospheric ozone between 1995 and 2030, using boundary conditions consistent with the recent World Meteorological Organization ozone assessment. We compare the Antarctic ozone recovery predictions of two simulations, one driven by meteorological data from a general circulation model (GCM), the other using the output of a data assimilation system (DAS), to examine the sensitivity of Antarctic ozone recovery predictions to the characteristic dynamical differences between GCM and DAS –generated meteorological data. Although the age of air in the Antarctic lower stratosphere differs by a factor of 2 between the simulations, we find little sensitivity of the 1995 -2030 Antarctic ozone recovery between 350 K and 650 K to the differing meteorological fields, particularly when the recovery is specified in mixing ratio units. Relative changes are smaller in the DAS -driven simulation compared to the GCM -driven simulation due to a surplus of Antarctic ozone in the DAS -driven simulation which is not consistent with observations. The peak ozone change between 1995 and 2030 in both simulations is ~20% lower than photochemical expectations, indicating that changes in ozone transport at 450 K between 1995 and 2030 constitute a small negative feedback. Total winter/ spring ozone loss during the base year (1995) of both simulations and the rate of ozone loss during August and September is somewhat weaker than observed. This appears to be due to underestimates of Antarctic Cl$_y$ at the 450 K potential temperature level.

1.Introduction

Observationsoverthelastdecadeindicatethattheburdenoforganicchlorineand bromine –containingcompoundsinthetropospherepeakedduringtheearly1990'sandarenow declining [WMO,2003] .Stratosphericinorganicchlorineconcentrationshaveleveledoff,and mayalsosoonbe observedtobedeclining [*Rinslandetal.* ,2003; *Waughetal.* ,2001] . Stratosphericchlorineandbromineconcentrationsareexpectedtodeclineoverthenextcentury providedthatthehalocarbonemissioncontrolsestablis hedbytheMontrealProtocoland associatedinternationalagreementsarefollowed [WMO,2003] .

Stratosphericozoneconcentrationsareexpectedtorespondtothesechlorinedecreases duetotheimportantroleofhalogensinozonephotochemistry [*Solomon*,1999] .Thepotential responseofAntarcticozoneisparticularlyinterestingbecauseofitshighsensitivitytoele vated halogenlevels.Inadditiontochangesinhalogenloading,thereareotherfactorswhichmay influenceAntarcticozonesuchaschangesinstratospherictemperatureanddynamicsduetothe buildupofgreenhousegases,thechemicaleffectsofcontinui ngincreasesinmethane(CH $_4$), nitrousoxide(N $_2$O),andwatervapor,andchangingstratosphericsulfateaerosolloading [*Shindelletal.* ,1998] .Itisthereforenotlikelythatozon erecoverywillbesimplyrelatedto decreasesinchlorine.Accountingfortheeffectsofthesevariousfactorschallengesthe scientificcommunityinterestedinpredictingtheresponseofthestratosphericozoneholeto futuredecreasesinstratospheric chlorine/bromineloading.

Therepresentationofstratospherictransportprocessesinamodel,particularlythose whichcontrolthehighlatitudes,willclearlyaffectitspredictionofozonerecovery.However, welackaquantitativeunderstandingofthis dependencyandthedegreeofuncertaintyin

recoverypredictionscausedbytheuncertaintiesinmodelingatmospherictransport.Thegoalof

thispaperistoimproveourunderstandingofthisrelationship.

Chemistryandtransportmodels(CTMs)ofthestrat ospheredonotgeneratetheirown

dynamicalfields.Insteadtheyrelyonexternally -suppliedmeteorologicaldatasets(temperatures,

winds,etc.)todrivetheCTMchemistryandtransportmodules.Themeteorologicaldatasetsare

generatedeitherbyafree -runninggeneralcirculationmodel(GCM)oradataassimilation

system(DAS)(ADASoptimallycombinesobservationalinformationwithGCMoutputto

produceostensiblymorerealisticmeteorologicaldatathanispossiblewithafree -runningGCM

[*CoyandSwinbank*,1997]).GCMandDASmeteorologicaldatasetshavecharacteristic

differenceswhichwillbediscussedbelow.

Inthispaper weintercomparetwodifferentsimulationsofAntarcticozonerecovery

madewiththeGlobalModelingInitiative(GMI)3DChemistryandTransportmodel [*Rotmanet

al.*,2001] .Theonlydifferencebetweenthetwosimulationsisthemeteorologicaldatadriv ing

modeltransport.Oneisdrivenbytheoutputoffree -runningGCM,andtheotherbyaDAS.All

otheraspectsofthemodelincludingeventhemodeladvectionalgorithmandnumberand

locationofverticallevels,remainthesame.Comparingsimulationsdri venbythesetwo

meteorologicaldatasetsteststhesensitivityofAntarcticozonerecoverypredictionstothe

characteristicdifferencesbetweenGCM -derivedandDAS -derivedmeteorologicaldatasets.

Insection2webrieflydescribetheGMImodel.Insec tion3weoutlinethemodel

experiments.Insection4weshowandinterprettheresultsofthesimulations.Weprovidea

summaryandconclusionsinsection5.

2.ModelDescription

The GMI 3D CTM was first described by *Rotman et al.* [2001]. Application of the model to the potential impacts of stratospheric aircraft emissions is presented in *Kinnison et al.* [2001]. The model was used to investigate the effects of stratospheric aircraft emissions on the occurrence of polar stratospheric clou ds (PSCs) in *Considine et al.* [2000].

The current study utilized two sets of meteorological information (horizontal winds, surface pressures, and temperature distributions) to drive the CTM. These datasets were generated by the Goddard Space Flight Center Data Assimilation Office and the Atmospheric Chemistry and Dynamics Branch. The first was generated from a run of the "Finite Volume" General Circulation Model (FVGCM), a new GCM jointly developed by NASA and th e National Center for Atmospheric Research (NCAR). This GCM combines the physical parameterizations of the NCAR CCM3 GCM [*Kiehl et al.*, 1998] with the *Lin and Rood* [1997] advection scheme (See http://polar.gsfc.nasa.gov/sci_research/fvdas/index.php) for details. The second set of meteorological data was generated by a recent version of the Goddard Earth Observing System Data Assimilation System (GEOS -DAS) [*Schubert et al.*, 1993], which uses the FVGCM to provide forecasts for the DAS. *Schoeberl et al*.[2003] provide a useful comparison of FVGCM and FVDAS characteristics.

Both sets of meteorological data were interpolated to the same hybrid sigma -pressure coordinate system for this study, following the technique used to create meteorological datasets for the Goddard Space Flight Center 3D CTM [*Considine et al.*, 2003]. The horizontal resolution of the coordinate system is 5 $^{\mathrm{o}}$ longitude by 4 $^{\mathrm{o}}$ latitude, with 28 vertical levels. The interface between sigma (terrain -following) and constant pressure horizontal surfaces occurs at 247.46 hPa. The model ex tends up to .43 hPa, about the top of the stratosphere.

The photochemical scheme has been upgraded from *Rotman et al.* [2001] with improvements described in *Douglass et al.*, "Radicals and reservoirs in the GMI chemistry and transport model: Comparison to measurements," submitted to Journal of Geophysical Research, 2003 (hereafter referred to as Douglass 2003). The PSC parameterization settings were changed from that described in *Considine et al.* [2000]. In this version, Type 1 PSCs were assumed to have a nitric acid trihydrate (NAT) composition instead of supercooled ternary sulfate (STS). This choice results from a desire to better represent the PSC characteristics of the Arctic, where recent observations by *Fahey et al.* [2001] show extensive NAT particle formation and denitrification, and the recent study of *Considine et al*. [2003], which showed that STS aerosols are ineffective denitrifiers of the Arctic polar vortex due to their small size. The WMO 2002 background sulfate aerosol distribution is also included, which catalyzes heterogeneous reactions with the same temperature dependence as STS aerosols. Thus the only Type 1b (liquid) PSC processes which are neglected in this parameterization are the swelling of the PSCs at low temperatures due to HNO_3 uptake, and their sedimentation.

3. Experiment Description

The two simulations using the GCM and DAS meteorological datasets will be referred to as the GMI_GCM and GMI_DAS simulations, respectively, for the remainder of this paper. The source gas boundary conditions used for the two simulations correspond to the MA2 scenario specified in Table 4B-1 of the WMO 2002 ozone assessment [WMO 2003]. The simulations were initialized similarly and spun up for five years at 1995 source gas boundary conditions. The simulations were then integrated forward in time for 36 years, through the year 2030. Halocarbon surface mixing ratios were specified from Table 4B-2 of the WMO assessment

report. CH_4 and N_2O mixing ratios were specified as scenario A2 of the International Panel on Climate Change 2001 report, also listed in Table 4B-3 of the WMO assessment.

The background sulfate aerosol distribution was specified using the WMO 2002 assessment aerosol dataset. The aerosols followed observed values from 1995 to 1999. Between 2000 and 2030, the aerosol distribution for 1997 was repeated annually.

One year of meteorological data was used to drive each simulation, and the year was recycled for each year of the simulation. The year of FVGCM data used in the GMI_GCM calculation was taken from a 50-year run of the FVGCM. The particular year was chosen on the basis of its relatively cold Arctic winter, for reasons unrelated to the work presented in this paper.

For both simulations the year of data used extends from July 1, through June 30. The FVDAS data corresponds to July 1, 1999 through June 30, 2000. Thus on each year of the 36 years simulation there is a discontinuity between June 30 and July 1 where there are relatively large changes in wind fields, etc. The analysis presented below does not appear to be affected by this discontinuity.

The model diagnostics used in the following analysis consist of species mixing ratios written out at 0Z every 3 days during 1995 and during 2030. The analysis also uses three-day average reaction rates, again written out at 0Z every 3 days.

4. Results

4.1 Dynamical Differences

There are substantial dynamical differences between the two sets of meteorological data used to drive the GMI_GCM and GMI_DAS simulations. One important difference is the strength of the stratospheric residual circulation. A good measure of residual circulation strength is the mean

age of stratospheric air, and how it is distributed in latitude and altitude. The mean age of the air at a particular latitude and altitude can be thought of as the average time for a parcel of air to travel from the ground to that latitude and altitude [*Hall and Plumb*, 1994; *Waugh and Hall*, 2002]. Figure 1 shows the vertical and meridional distribution of the mean age of air calculated from simulations using the GCM (Figure 1a) and DAS (Figure 1b) wind fields described above. Figure 1c shows the difference between the two age distributions, and Figure 1d compares the simulated mean ages with values inferred from NASA ER-2 aircraft observations of CO_2 [*Boering et al.*, 1996]. Figure 1a shows that the GCM meteorological data produces a mean age of ~5.5 – 6 years in the upper stratosphere. The DAS-derived upper stratospheric mean age shown in Figure 1b is ~2 years younger. In the upper stratosphere the GCM-derived mean age is in much better agreement with observationally-derived estimates. Figure 1d shows that this is also the case in the lower stratosphere [*Hall et al.*, 1999; *Waugh et al.*, 2001]. The mean age differences shown in Figure 1 are typical of GCM-based and DAS-based circulations. In general, residual circulations inferred from analyzed meteorological data are too vigorous, producing young stratospheric air. [*Considine et al.*, 2003; *Schoeberl et al.*, 2003; *Weaver et al.*, 1993].

Distributions of long-lived tracers such as N_2O and CH_4 can also provide information about transport differences between the GMI_GCM and GMI_DAS simulations. Figures 2a and 2b show equivalent-latitude averaged N_2O in September on the 650K and 450K potential temperature surfaces, respectively, as a function of equivalent latitude, from the GMI_GCM and GMI_DAS simulations. The figure also shows equivalent latitude averaged N_2O distributions derived from Cryogen Limb Array Etalon Spectrometer (CLAES) satellite observations made during September, 1992, at 650K and 450K [*Roche et al.*, 1996]. At 450K, Airborne Tunable

LaserAbsorptionSpectrometer(ATLAS)observationsmadeduringtheSeptember,1987flights

oftheAirborneAntarcticOzoneExperiment(AAOE)andtheOctober,1994flightsofthe

AirborneSouthernHemisphereOzoneExperiment(ASHOE   )areincludedaswell   [*Loewenstein*

etal,1989;   *Loewensteinetal*,1990]   .

ThesimulatedandobservedN2Odistributionsallexhibitthefamiliar"rollercoaster"

patterncausedbylowerstratosphericdynamicalprocessesatboth450Kand650K.At650K,

thegradientseparatingthetropicsfromthemidlatitudesissubstantiallyweakerintheGMI_DAS

simulationthanineithertheCLAESobservationsortheGMI_GCMsimulation.Thegradients

separatingthemidlatitudesfromthepolarvortexaresimilarinboth   simulationsat650Kandare

weakerthanobserved.Theweakergradientsindicatethatthemeridionalmixingbetweenthe

vortexandmidlatitudesistoostrongrelativetothedescentrateofairwithinthevortexinboth

simulations.

At450Kthesubtro   picalN2Ogradientsseparatingthetropicsfromthemidlatitudesare

similarinbothsimulationsandareweakerthanareobserved.AthighlatitudestheGMI_GCM

N2OdistributionsagreebetterwithobservationsthantheGMI_DASsimulation,suggestinga

somewhatmoreisolatedandrealisticrepresentationofthepolarvortex.

Overall,theGMI_GCMsimulationmoreconvincinglyreproducesobservedN2O

distributions.ThedifferencesbetweenthesimulatedN2Odistributionsareconsistentwiththe

youngerageof   high-latitudeairintheGMI_DASsimulationandfurtherillustratea

characteristicproblemwithCTMsimulationsdrivenbyDAS   -generatedwindfields.Further

evaluationofthedifferenteffectsofthetransportfieldsonstratospherictracerdistributions   is

providedinStrahan,S.E.andA.R.Douglass,"Evaluatingthecredibilityoftransportprocesses

intheGlobalModelingInitiative3Dmodelsimulationsofozonerecovery," *Journalof*

GeophysicalResearch –Atmospheres,submittedarticle,2003 (hereafte rreferredtoasSD2003).

Anotherimportantdifferencetoconsideristheoccurrenceoftemperatureslowenoughto

provokeformationofPSCs.Theoccurrenceoftheselowtemperaturesinthetwosimulationsis

showninFigure3.Figure3ashowsthesizeof theAntarcticregionbelow195K(the

approximatetemperaturebelowwhichPSCscanform)asafunctionofdayofyearandpotential

temperatureintheGMI_GCMsimulation.Theareaisexpressedasafractionofthetotalglobal

area.Figure3bshowsthes ameplotfortheGMI_DASsimulation,andFigure3cshowsthe

differencebetweenthetwo.Figures3aand3bdemonstrateaqualitativelysimilarmorphology,

withthecoldesttemperaturesoccurringearlierintheyearathigherpotentialtemperatures.

Figure3cshowsthatdifferencesbetweenthetwosimulationsintheoccurrenceofcold

temperaturesisnotlarge.Inthelowerstratosphere(~450K)theGMI_DASsimulationhasa

slightlylargercoldpoolthroughoutmostoftheyear,althoughduringdays~210t o~240the

GMI_GCMcoldpoolislargerby~10%.Thesimilarityoftheoccurrenceofcoldtemperatures

intheGMI_DASandGMI_GCMsimulationsallowsforamorespecifictestofthesensitivityof

recoverypredictionstodynamicaldifferencesbetweenthetw osimulations.

4.21995- 2030ChangesinOzone

Figure4showsthechangeinAntarcticozonemixingratiosinresponsetosourcegas

forcingbetween1995and2030asafunctionofdayofyearandpotentialtemperatureinthe

GMI_GCM(Figure4a)andGMI_DAS (Figure4b)simulations.Thefiguresshowanaverage

overequivalentlatitudes"poleward"of -65°equivalentlatitude.Wewillusesuchaverages

throughoutthispapertoprovideameasureofaverageconstituentbehaviorintheAntarctic.

Figures4aand4b showsimilarchangesinAntarcticozoneinthesetwosimulations.Inthe

GMI_GCM simulation, the peak ozone increase of 0.76 ppmv occurs at ~500K on Julian day 278, in early October. At 450K, the peak occurs 3 days later and reaches 0.7 ppmv. In the GMI_DAS simulation, the peak ozone increase of 0.70 ppmv also occurs at 500K on day 278. At 450K, the peak increase is 0.66 ppmv. Thus, the GMI_GCM peak is ~6% larger than in the GMI_DAS at 450K and ~8.5% larger at 500K. The Antarctic ozone recovery predictions appear to display little sensitivity to the substantial differences in the meteorological data which lead to the age differences shown in Figure 1. Larger differences between the GMI_GCM and GMI_DAS simulations are shown in Figures 5a and 5b, which show the percentage differences in Antarctic ozone between 1995 and 2030 in the GMI_GCM (5a) and GMI_DAS (5b) simulations. In contrast to Figure 4, the peak 1995-2030 change in Antarctic ozone of ~40% occurs at 450K in the GMI_GCM simulation, while there is a smaller increase of ~28% in the GMI_DAS simulation at 400K. Peak relative changes occur at about the same day of the year, but occur ~50K and ~100K lower in potential temperature than the locations of the peak mixing ratio differences in the GMI_GCM and GMI_DAS simulations, respectively.

The relative GMI_GCM peak shown in Figure 5a is ~43% larger than the GMI_DAS peak shown in Figure 5b even though the peak 1995-2000 mixing ratio differences are similar because of differences between the base years (1995) of the simulations. Figure 6 compares Antarctic ozone mixing ratios from the two simulations for the base year on the 450K (Figure 6a), 550K (Figure 6b), and 650K (Figure 6c) potential surfaces. Also included in the figure are observed values from 1992 (red crosses), 1993 (blue crosses), and 1994 (green crosses) version 5 MLS measurements [*Froidevaux et al.*, 1996; *Livesey et al.*, 2003], and 1992 version 9 CLAES observations [*Bailey et al.*, 1996]. Both simulations have the same general morphology, with peak ozone occurring in the winter and minima during the late spring. However, there is

generallymoreAntarcticozoneintheGMI_DASsimulation.Figure6ashowsthatthereisupto ~1.0ppmvmoreozoneintheGMI_DASsimulationat450KthanintheGMI_GCMsimulation. ThehigherozonemixingratiosintheGM I_DASsimulationproducethesmallerrelative1995 - 2030differencesshowninFigure5b.

TheGMI_GCMsimulationagreesbetterwiththeMLSozonemeasurementsat450K and550KthanGMI_DAS.At650K,bothmodelsimulationsexhibitanannualcyclewhichis morepronouncedthanseenintheobservations.NotethattheMLSobservationsat450Ksuffer fromaninstrumentalartifactwhichresultsinhigherozonemixingratiosduringthemiddleofa yawcyclethanatthebeginningorend.Thisartifactisparticu larlynoticeableduringthewinter yawcycleof1993inFigure6a.Thecauseoftheartifactisnotwellunderstood [*Froidevauxet al.*,1996] ,butthefewtenthsofapartpermillionvariationdoesnotseriouslyaffectthis qualitativecomparison.Theartifactisknowntobesmallerinversion5retrievalsthanpreviously [*William G.Read,privatecommunication* ,2003].Therearesignificantdifferencesbetweenthe 1992MLSandCLAESobservationsduringthefallandwinteryawcycles.Thismaybedueto theexistenceofheavyPSCsduringthistime,whichinterferewiththeCLAESr etrieval.Atother timesofyeartheCLAESandMLSobservationsagreewellwitheachother.

Althoughthe1995 -2030increaseinozoneisnotverysensitivetothedynamical differencesbetweenthetwosimulations,thesimulationofthebaseyearis.Thisi sinteresting becauserelativedifferencesaretypicallycomparedinassessmentexercises,ratherthanabsolute (mixingratio)differences.Suchanapproachmayintroducesubstantialintermodelvariability intoanassessmentexerciseasaconsequence,even incaseswherethemodelresponsesare similarinabsoluteterms.

We compare in the next section the evolution of ozone over the course of the winter/spring season to determine the manner in which ozone concentrations evolve and are determined by springtime chemical and dynamical influences. This will help explain the low sensitivity of the 1995-2030 increase in ozone to the dynamical differences between the two simulations.

4.3 Evolution of ozone in 1995

We choose to examine in detail the evolution of Antarctic ozone from winter through spring in the base year of the simulations at 450 K potential temperature level, because peak 1995-2030 ozone changes in both simulations occur within 50 K of this surface, with the changes expressed either as a mixing ratio or a percentage difference. We also use July 1 as a reference point to compare specifically the springtime ozone changes. The solid line in Figure 7a shows the change in Antarctic ozone (i.e., the loss of ozone) after July 1 in the GMI_GCM simulation at 450 K. Two other lines are also shown on this plot. The dashed line shows the integrated chemical loss of ozone after July 1, calculated from model chemical rate diagnostic output. The dash-dot line shows the difference between the actual loss of ozone and the integrated chemical loss of ozone, which indicates the influence of transport. The red, blue, and green crosses in Figure 7a show changes in Antarctic ozone mixing ratios after July 1 calculated from ozone observations made in 1992, 1993, and 1994, respectively, by the Microwave Limb Sounder (MLS) instrument.

Figure 7a shows that over the course of the winter and spring seasons the GMI_GCM simulation has a maximum loss of ozone of ~1.9 ppmv. The solid line showing the actual ozone loss in the model tracks very close to the dashed line showing integrated chemical loss through ~day 280 (early October). This indicates that at this potential temperature the evolution of ozone

isdominatedbychemicallossandozonetransportplaysaminorrole - through day280,Figure 7asuggeststhattransporthasreducedozonelossby~9%.Notehoweverthatthisfactdoesnot meanthattransportisunimportant –justthatchangesinozoneduetothetransportofozone itselfaresmallcomparedtochangesinozonedue toin -situphotochemistry.Thein situ photochemistrymaybesubstantiallyinfluencedbytransport,forinstanceofCl $_y$.Afterday280 netozoneloss(solidline)remainssteadywhiletheintegratedchemicallosstermcontinuesto dropbyabout0.5ppmvt hroughtheendoftheyear.Ozoneisthusbeingtransportedintothe regionduringthistimetobalancethecontinuingchemicalloss.Thefactthatozonetransportis smallduringtheAugust/Septembertimeframeisconsistentwiththeresultsof *WuandDe ssler* [2001],whichcomparedozonelossat465KobservedbyMLSwithestimatesofchemicalloss basedonMLSobservationsofClOduringAugustandSeptemberof1992,1993,and1994.

Comparisonofthesimulatedozone inFigure7awiththeMLSobservationsshowsthat theozonelossisabout20%lowerthantheaverageobservedozonelossduring1992,1993,and 1994.Also,averagedovertheUARSspringtimeyawcycle,thesimulatedrateofchang eof ozoneis~30%smallerthanisobserved -~28.5ppbv/daycomparedtotheobserved~41.4 ppbv/day(weaverageovertheyawcycletoremovetheeffectsoftheinstrumentalartifact discussedabove).

Figure7bshowsthesamecomparisonasinFigure7afor theGMI_DASsimulation.The figureshowsthattherearestrongsimilaritieswiththeGMI_GCMresultsshowninFigure7b. Themaximumlossofozoneis~2.2ppmvataboutday330.Althoughtransportcausesaninitial deviationfromthechemicallossinlateJuly(~day200),simulatedozonelossisvirtually identicaltothechemicallossbyday280,andapproximatelyparallelstheintegratedchemical lossthroughaboutday300(lateOctober).IncontrasttotheGMI_GCMresults,duringthelast

two months of the year, model ozone loss exceeds the integrated chemical loss, implying that transport acts to reduce ozone after about day 300 (Note that transport is acting to reduce Antarctic ozone concentrations from day 200 on, but the net effect of transport is near zero through day 300). Kinematic back-trajectory calculations of high equivalent latitude parcels initialized at 450K indicate that this is due to transport of some air with smaller ozone mixing ratios to the 450K from below.

As above, the overall loss is somewhat low compared to observations. The ozone loss rate of ~26.1 ppbv/day during the August/September time period is also substantially weaker than observed and slightly weaker than in the GMI_GCM simulation. Interestingly, Figure 7b shows that ~4 ppbv/day of the loss rate during August/September is due to transport, or about 16%. Without the transport contribution, the chemical loss rate is ~23% smaller than the GMI_GCM loss rate. The total chemical loss is 1.9 ppmv, which is about 18% smaller than the chemical loss in the GMI_GCM simulation.

We next examine in more detail the photochemistry of the two simulations to determine the causes of these differences.

4.4 Photochemisty in 1995

The primary deficiency of the model calculations shown in Figure 7 is the weak ozone loss compared to the MLS observations in the August/September timeframe, particularly in the GMI_DAS simulation. Virtually all of the ozone destruction (>93%) at this time in the two simulations is caused by catalytic cycles involving Cl_y and Br_y radical species.

We refer to the sum of the radical ClO and its nighttime reservoir Cl_2O_2 as "active chlorine," and denote it by the symbol Cl_x. Figure 8a shows high-latitude averaged Cl_x and Cl_y on the 450K surface between days 100 and 350 from both simulations. The figure shows that Cl_y

peaks in August in both simulations with values of ~2.3 ppbv for GMI_GCM and ~1.8 ppbv for GMI_DAS – ~22% less. The larger Cl_y mixing ratios in the GMI_GCM simulation result in larger Cl_x mixing ratios for this simulation as well. Figure 8b compares the ratio Cl_x/Cl_y in the two simulations. Peak Cl_x activation exceeds 85% in both simulations. The ratio is similar during August/September, dropping from ~80% to ~60% by mid-September. The similarity of the ratio indicates that the weaker GMI_DAS ozone loss during this time shown in Figure 7b is due to lower Cl_y at 450K, rather than differences in chlorine activation.

Also shown in Figure 8a is an estimate of Cl_y derived from CLAES N_2O observations made during the Antarctic winter/spring of 1992 using the Cl_y/N_2O relationship derived in *Woodbridge et al.*, [1995]. During September (days ~244–273), the Cl_y in the GMI_GCM simulation agrees reasonably well with the observational estimates although observationally-inferred Cl_y is apparently increasing during this time while the simulated Cl_y is beginning to drop from a winter peak. The Cl_y in the GMI_DAS simulation is low by ~0.5 ppbv. The observational estimates suggests that Cl_y increases until December, which is contrary to the decreasing trend in both simulations. This late-year discrepancy has little impact on simulated ozone loss because the Cl_x/Cl_y ratio falls to very low values by this time due to the return of sunlight and warm temperatures to high latitudes. More detail on the evolution of high latitude tracer concentrations during the Southern Hemisphere springtime is given in SD2003.

We can also estimate Cl_y from the lower stratospheric high latitude N_2O observations made during the AAOE and ASHOE expeditions which are shown in Figure 2. Figure 9 shows these observed estimates of Cl_y and simulated Cl_y at 450K as a function of equivalent latitude. All three of the observational estimates exceed both the GMI_GCM and GMI_DAS simulations throughout the southern hemisphere. At midlatitudes both simulations are quite a bit lower than

the observational estimates, likely due to the very weak meridional gradient across the subtropics. At high latitudes the GMI_GCM simulated Cl_y is ~15% low, while the GMI_DAS underestimate at high latitudes is ~30%.

Wu and Dessler [2001] estimate from MLS ClO observations vortex-averaged Cl_x mixing ratios of ~2–2.5 ppbv at 465 K during the late August/early September period in 1992, 1993, and 1994. Figure 8a shows that Cl_x in the GMI_GCM simulation is about 15% to 20% lower than this estimate, and Cl_x in the GMI_DAS simulation is about 30% to 35% low. These deficits are consistent with the Cl_y comparisons shown above and could account for the weak August/September loss rate seen in the GMI_GCM and GMI_DAS simulations.

Figures 8 and 9 show that the in-situ photochemistry which controls Antarctic lower stratospheric ozone loss is affected by the differences in atmospheric transport which lead to the age discrepancies shown in Figure 1. Some combination of higher meridional mixing and/or lower vertical descent of air at high latitudes in the GMI_DAS simulation results in lower Cl_y mixing ratios at 450 K than in the GMI_GCM simulation. The result is about 20% lower total chemical ozone loss and a correspondingly smaller chemical ozone loss rate during August/September. Similarly, both Cl_x and Cl_y in the GMI_GCM simulation appear to be about 20% lower than observed values. These differences are relatively modest considering that the age of lower stratospheric Antarctic air differs by about a factor of 2 in the two simulations.

4.5 Chemistry and transport contributions to 1995–2030 ozone change

In section 4.2 above we showed that the peak 1995-2030 increase in Antarctic ozone at 450 K in the GMI_GCM simulation is only ~6% larger than the peak increase in the GMI_DAS simulation, despite the substantial dynamical differences in the meteorological data driving the two simulations discussed in section 4.1. Section 4.3 showed that the dynamical differences

cause~20%differencesbetweentheGMI_GCMandGMI_DAS simulationsinthespringtime

chemicalozonelossduringthebaseyearofthesimulations,duelargelytotheeffectsof

transportonCl$_y$(andbyimplication,Br$_y$).Totrytodeterminewhythepeak1995 -2030increases

inthetwosimulationsdifferby~6% whilespringtimeozonelossforthebaseyearsdifferby

~20%,wenowexaminetheindividualchemistryandtransportcontributionstothe1995 -2030

ozonechange.

Figure10ashowsthehighlatitudewinter/springozonelossintheGMI_GCMand

GMI_DASsimulat ionsat450Kfor1995(solidlines),2030(dashedlines)andthedifference

between1995and2030(dashed -dotlines).Thefigureshowsthatwhilethewinter/springozone

lossesintheGMI_GCMandGMI_DASsimulationsdifferintimingandmagnitude,the19 95-

2030differenceinozonelossineachofthesetwosimulationsisverysimilar,consistentwiththe

differencesshowninFigure4above.Peakvaluesofthedifferenceare0.56ppmvonday281in

theGMI_GCMsimulationand0.51ppmvonday275intheGM I_DASsimulation.Thus,the

GMI_GCM1995 -2030peak"recovery"ofAntarcticozoneisslightlylessthan10%largerthan

therecoveryintheGMI_DASsimulation.

Figure10bshowsthewinter/springchemicallossofozonein1995(solidblue(GCM)

andred(D AS)lines)and2030(dashedblueandredlines)inthetwosimulations,inadditionto

the1995 -2030changeinwinter/springchemicallossat450Kforthesimulations(dash -dotblue

andredlines).Onthedaysofthepeak1995 -2030changeinozonelossfo rthetwomodel

simulationsshowninFigure10a,the1995 -2030changeinchemicallossis0.69ppmvforthe

GMI_GCMsimulationand0.66ppmvfortheGMI_DASsimulation.Whenonlythechangein

chemicallossisconsidered,theGCM -drivensimulationisjust 4.5%largerthantheDAS -driven

simulation.

At the same time the blue and red solid lines in Figure 10b show that the 1995 chemical loss from July 1 through the day of peak recovery is ~2.1 ppmv in the GMI_GCM simulation and ~1.5 ppmv in the GMI_DAS simulation. So, even though the GCM-driven simulation has a chemical ozone loss that is ~38% larger than the DAS-driven simulation at this time, the change in the chemical ozone loss between 1995 and 2030 is only slightly larger (4.5%) than the DAS-driven simlation. This will be discussed further below.

Figure 10c shows the effects of transport on ozone loss in 1995 (solid lines) and 2030 (dashed lines) for the GMI_GCM (blue) and GMI_DAS (red) simulations. It also shows the 1995-2030 difference (dash-dot lines) for each of the simulations. The 1995-2030 differences are relatively similar between the two simulations, with the GMI_DAS transport contribution slightly more negative than GMI_GCM. Note that since the 1995-2030 change in ozone transport is due entirely to changes in ozone gradients in the Antarctic (the wind fields themselves are the same every year), a negative contribution from transport is expected due to weaker ozone gradients in 2030 compared to 1995. On the day of peak ozone recovery (Figure 9), the effect of changes in transport is to reduce the recovery peak by ~19% in the GMI_GCM simulation and ~23% in the GMI_DAS simulation.

Figure 10 shows that the effect of changes in the role of ozone transport between 1995 and 2030 is to create a larger difference in the ozone recovery of these two simulations, rather than a smaller difference. In the absence of the transport effects, the difference between the two simulations would simply be that of the 1995-2030 changes in chemical ozone loss -~4.5%. Ozone transport is therefore not obscuring a larger difference between the simulations in the response of Antarctic photochemistry to the 1995-2030 changes in source gas forcing.

Figures 7a and 7b show that the bulk of the springtime ozone loss in bo   th simulations occurs between days 220 and 280. The decreases in Cl_x and Cl_y from 1995 to 2030 that occur during this time period will determine how ozone changes due to photochemistry between 1995 and 2030. Figure 11 shows these decreases in Cl_x and Cl_y from 1995 to 2030 for both the GMI_GCM and GMI_DAS simulations. Figure 11 shows that the 1995   -2030 change in Cl_y in the GMI_DAS simulation is about 10% smaller than the corresponding change in the GMI_GCM simulation. This is about half of the amount by   which 1995 Cl_y in the GMI_DAS simulation differs from the GMI_GCM simulation. Figure 11 also shows that the 1995   -2030 change in Cl_x in the GMI_DAS simulation is about the same as corresponding change in the GMI_GCM simulation. This implies that in the GMI   _DAS simulation the Cl_x/Cl_y ratio has decreased between 1995 and 2030, making the overall decline in Cl_x about the same as in the GMI_GCM simulation. Although it is not clear exactly why the Cl_x/Cl_y ratio decreases in the GMI_DAS simulation more than in t   he GMI_GCM simulation, this behavior explains the similarity of the 1995   -2030 change in chemical ozone loss in the two simulations.

5. Summary and Conclusions

We have used the GMI 3DCTM to simulate ozone recovery over the the 1995   –2030 time period using   two different representations of atmospheric transport processes. We have compared Antarctic ozone recovery predictions generated in these two simulations to evaluate the sensitivity of the recovery predictions to the characteristic differences between GC   M and DAS meteorological datasets.

The simulation driven by the GCM meteorological fields realistically captures the age of air distribution of the stratosphere, while the age of stratospheric air in the DAS   -driven simulation is up to 2.5 years younger th   an observed. The GCM   -driven simulation also has a

morerealisticrepresentationoflonglivedtracespecies,asdemonstratedbythecomparisonof simulatedandobservedN $_2$O.Bothsimulationshavesimilarcoldpoolregionsinthepolar southernhemisphere, afactwhichmakestheintercomparisonofthesimulationsamoredirect testofdynamicalsensitivitythanwouldotherwisebethecase.

Despitethesubstantialdynamicaldifferencesinthetwosimulations,the1995 -2030 responseofozonemixingratiosbet ween350Kand650KatAntarcticlatitudestochangesin tracegasforcingisverysimilar.Thisindicatesthatthedynamicaldifferencesbetweenthe simulationsdonotstronglyinfluencethe1995 -2030ozonechange.Onecannotthereforeargue thataDAS -generatedmeteorologicaldataset,oranysetwhichunderestimatesstratosphericage, isautomaticallyinappropriateformakingozonerecoverycalculations.Differencesbetween long-livedtracersintheAntarcticlowerstratosphereprovideabetterindicat orofresponseto changesinsourcegasboundaryconditions.

TherelativeresponseofAntarcticozonetosourcegaschangesbetween1995and2030 showslargerdifferencesbetweenthetwometeorologicaldatasetsandandisstrongerinthe simulationdri venbyGCMoutputduetolowerAntarcticozoneconcentrationsinthebaseyear ofthesimulation.Theutilityofrelativeozonechangeasameasureofrecoverytherefore dependsonhowwellthecurrentyearissimulated.

ThelowerozoneintheGMI_GCMsim ulationisinbetteragreementwithobservations. Intheabsenceofotherfactorswhichcouldaffectrecovery,suchaschangesinstratospheric temperaturesorwatervapor,therecoverypredictiontheGMI_GCMsimulationwouldbemore credibleasaresult.

Antarcticwinter/springozonelossat450Kinbothsimulationsisdrivenprimarilyby photochemistrythroughtheendofOctober,andozonetransporttoorfromthevortexat450K

playsonlyasmallandsimilarroleduringthistime.Thisresultisconsi   stentwithobserved behavior.Totalozonelossinbothsimulationsagreesreasonablywellwithobservationsinboth simulations,buttherateofozonelossduringtheAugust/Septembertimeperiodisweak.The weaklossappearstobeexplainedbylowCl$_x$athighlatitudes,whichisdueinlargeparttolow Cl$_y$.

Theseresultshaveimplicationsforthetypesofmodelintercomparisonsusedinthe WMOassessmentreports.Theseassessmentstypicallypresentmodelresultsintermsofrelative ratherthanabs olutedifferencesfromsomebaseyear,forinstance1980(seeforexampleFigure 4-42ofWMO [2003]).Ifabsolutedifferenceswereusedinsteadtheintermodelvariabilityseen insuchfiguresmaybesignificantlyreduced.

References

WMO(WorldMeteorological Organization),Scientificassessmentofozonedepletion:2002, GlobalOzoneResearchandMonitoringProject -ReportNo.47,498pp.,Geneva,2003

Bailey,P.L.,etal.,Comparisonofcryogeniclimbarrayetalonspectrometer(CLAES)ozone observationswith correlativemeasurements, *JournalofGeophysicalResearch - Atmospheres*, *101*(D6),9737 -9756,1996.

Boering,K.A.,S.C.Wofsy,B.C.Daube,H.R.Schneider,M.Loewenstein,andJ.R.Podolske, Stratosphericmeanagesandtransportratesfromobservationsofcar bondioxideand nitrousoxide, *Science*,*274* (5291),1340 -1343,1996.

Considine,D.B.,A.R.Douglass,P.S.Connell,D.E.Kinnison,andD.A.Rotman,Apolar stratosphericcloudparameterizationfortheglobalmodelinginitiativethree -dimensional modelandi tsresponsetostratosphericaircraft, *JournalofGeophysicalResearch - Atmospheres*, *105*(D3),3955 -3973,2000.

Considine,D.B.,S.R.Kawa,M.R.Schoeberl,andA.R.Douglass,N2OandNOyobservationsin the1999/2000Arcticpolarvortex:Implicationsfortr ansportprocessesinaCTM, *JournalofGeophysicalResearch -Atmospheres*,*108* (D5),4170, doi:10.1029/2002JD002525,2003.

Coy,L.,andR.Swinbank,Characteristicsofstratosphericwindsandtemperaturesproducedby dataassimilation,*JournalofGeophysical Research -Atmospheres*,*102*(D22),25763 - 25781,1997.

Fahey,D.W.,etal.,ThedetectionoflargeHNO3 -containingparticlesinthewinterarctic stratosphere, *Science*, *291*(5506),1026 -1031,2001.

Froidevaux, L., et al., Validation of UARS microwave limb sounder ozone measurement, *Journal of Geophysical Research - Atmospheres*, *101* (D6), 10017 -10060, 1996.

Hall, T.M., and R.A. Plumb, Age as a Diagnostic of Stratospheric Transport, *Journal of Geophysical Research -Atmospheres*, *99* (D1), 1059 -1070, 1994.

Hall, T.M., D.W. Waugh, K.A. Boering, and R.A. Plumb, Evaluation of transport in stratospheric models, *Journal of Geophysical Research -Atmospheres*, *104*(D15), 18815 -18839, 1999.

Kiehl, J.T., J.J. Hack, G.B. Bonan, B.A. Boville, D.L. Williamson, and P.J. Rasch, The National Center for Atmospheric Research Community Climate Model: CCM3, *Journal of Climate*, *11*(6), 1131 -1149, 1998.

Kinnison, D.E., et al., The Global Modeling Initiative assessment model: Application to high-speed civil transport perturbation, *Journal of Geophysical Research Atmospheres*, *106* (D2), 1693 -1711, 2001.

Lin, S.J., and R.B. Rood, An explicit flux-form semi-Lagrangian shallow -water model on the sphere, *Quarterly Journal of the Royal Meteorological Society*, *123*(544), 2477 -2498, 1997.

Livesey, N.J., W.G. Read, L. Froidevaux, J.W. Waters, M.L. Santee, H.C. Pumphrey, D.L. Wu, Z. Shippony, and R.F. Jarnot, The UARS microwave limb sounder version 5 dataset: Theory, characterization, and validation, *Journal of Geophysical Research -Atmospheres*, *108*(D13), doi:10.1029/2002JD002273, 2003.

Loewenstein, M., J.R. Podolske, K.R. Chan, and S.E. Strahan, Nitrous -Oxide as a Dynamical Tracer in the 1987 Airborne Antarctic Ozone Experiment, *Journal of Geophysical Research-Atmospheres*, *94* (D9), 11589 -11598, 1989.

Loewenstein, M., J. R. Podolske, and S. E. Strahan, Atlas Instrument Characterization -Accuracy of the Aase and Aaoe Nitrous -Oxide Data Sets, *Geophysical Research Letters*, *17*(4), 481-484, 1990.

Rinsland, C. P., et al., Long -term trends of inorganic chlorine fr omground -based infrared solar spectra: Past increases and evidence for stabilization, *Journal of Geophysical Research -Atmospheres*, *108*(D8), 4252, doi:10.1029/2002JD003001, 2003.

Roche, A. E., et al., Validation of CH4 and N2O measurements by the cryogenic limb array etalon spectrometer instrument on the upper atmosphere research satellite, *Journal of Geophysical Research -Atmospheres*, *101* (D6), 9679 -9710, 1996.

Rotman, D. A., et al., Global Modeling Initiative assessment model: Model description, integration, and testing of the transport shell, *Journal of Geophysical Research -Atmospheres*, *106*(D2), 1669 -1691, 2001.

Schoeberl, M. R., A. R. Douglass, Z. X. Zhu, and S. Pawson, A comparison of the lower stratospheric age spectra derived from a general circulation mo delandtwodata assimilation systems, *Journal of Geophysical Research -Atmospheres*, *108*(D3), 4113, doi:10.1029/2002JD002652, 2003.

Schubert, S. D., R. B. Rood, and J. Pfaendtner, An Assimilated Dataset for Earth -Science Applications, *Bulletin of the America n Meteorological Society*, *74*(12), 2331 -2342, 1993.

Shindell, D. T., D. Rind, and P. Lonergan, Increased polar stratospheric ozone losses and delayed eventual recovery owing to increasing greenhouse -gas concentrations, *Nature*, *392* (6676), 589 -592, 1998.

Solomon, S., Stratospheric ozone depletion: A review of concepts and history, *Reviews of Geophysics*, *37* (3), 275 -316, 1999.

Waugh, D. W., D. B. Considine, and E. L. Fleming, Is upper stratospheric chlorine decreasing as expected?, *Geophysical Research Letters*, *28*(7), 1187-1190, 2001.

Waugh, D. W., and T. M. Hall, Age of stratospheric air: Theory, observations, and models, *Reviews of Geophysics*, *40*(4), 1010, doi:10.1029/2000RG000101, 2002.

Weaver, C. J., A. R. Douglass, and R. B. Rood, Thermodynamic Balance of 3-Dimensional Stratospheric Winds Derived from a Data Assimilation Procedure, *Journal of the Atmospheric Sciences*, *50*(17), 2987-2993, 1993.

Woodbridge, E. L., et al., Estimates of Total Organic and Inorganic Chlorine in the Lower Stratosphere from in-Situ and Flask Measurements During Aase-Ii, *Journal of Geophysical Research-Atmospheres*, *100*(D2), 3057-3064, 1995.

Wu, J., and A. E. Dessler, Comparisons between measurements and models of Antarctic ozone loss, *Journal of Geophysical Research-Atmospheres*, *106*(D3), 3195-3201, 2001.

FigureCaptions

Figure1:MeanageofairintheGMICTMasafunctionoflatitudeandpressure.Topleft   -mean ageusingFVGCMmeteorologicaldata.Topright   -meanageusingFVDASmeteorological data.Bottomleft   -meanagedifferen   ce,FVGCM –FVDAS.Bottomright:Meridional dependenceat56hPaofmeanageintheFVGCM(solidline)andFVDAS(dashedline) simulations,comparedwithmeanageestimatesmadeusingaircraftCO_2observations(asterisks showthemeanagefromobservation   s,anddiamondsshowtheuncertaintyrange).

Figure2:ObservedandsimulatedN $_2$Oonthe:a.650Kandb.450Kpotentialtemperature surfacesasafunctionofequivalentlatitude.Solidblueline   –N $_2$OfromGMI_GCMsimulation, averagedovertheSeptembe   r1 –September18timeperiod.Solidredline   -N $_2$Ofrom GMI_DASsimulation,averagedovertheSeptember1   –September18timeperiod.Magenta asteriskswitherrorbars:equivalent   -latitudeaveragedN $_2$OfromtheCLAESinstrument, averagedfromSeptember   1toSeptember18.Errorbarsshow±1standarddeviationofall observedvaluesconstitutingtheaverage.Greendiamonds   –equivalentlatitudeaveragesof ALIASN $_2$OobservationsmadeduringSeptember,1987aspartoftheAAOE.Blackdiamonds –equivale ntlatitudeaveragesofALIASN $_2$OobservationsmadeduringOctober,1994aspartof ASHOE.

Figure3:ColdpoolareasintheGMI_GCMandGMI_DASsimulations.a.Coldpoolareainthe GMI_GCMsimulationasafunctionofdayofyearandpotentialtemperature   .Theareabelow 195Kintheextratropicalsouthernhemisphereisexpressedasapercentageofthetotalsurface areaoftheEarth.b.Sameasina,butfortheGMI_DASsimulation.c.Differenceinarea

betweentheGMI_DASandGMI_GCMsimulations.Apos itivenumbermeansalargerpoolin theGMI_DASsimulationandhence,alargerregionoftemperaturesbelow195K.

Figure4:ChangeinAntarcticozone(ozoneaveragedoverequivalentlatitudespolewardof 65°S)between1995and2030asafunctionofdayo fyearandpotentialtemperature,inmixing ratiounits.a.DifferencebetweenAntarcticozonein2030and1995intheGMI_GCM simulation.b.DifferencebetweenAntarcticozonein2030and1995intheGMI_DAS simulation.

Figure5:ChangeinAntarcticozo ne(ozoneaveragedoverequivalentlatitudespolewardof 65°S)between1995and2030asafunctionofdayofyearandpotentialtemperature,inpercent. a.DifferencebetweenAntarcticozonein2030and1995intheGMI_GCMsimulation.b. Differencebetwee nAntarcticozonein2030and1995intheGMI_DASsimulation.

Figure6:Antarcticozonemixingratioinpartspermillionbyvolumeasafunctionofdayofyear during1995ata.450K,b.550K,andc.650KintheGMI_GCM(solidline)andGMI_DAS simulations(dashedline)simulations.Alsoshownareaveragesofobservedozonevaluesfor equivalentlatitudespolewardof65 °SoneachpotentialtemperaturesurfacefromtheMLS instrumentin1992(redcrosses),1993(bluecrosses),and1994(greencrosses), andtheCLAES instrument(magentacrosses).

Figure7:Antarcticozonelossinthea.GMI_GCMandb.GMI_DASsimulationsfor1995at 450K.OzonelossisdefinedasthechangeinozonesinceJuly1.Solidline:simulatedozone

loss.Dashedline:integra tedchemicalozoneloss(seetextforexplanation).Dash -dotline:

simulatedlossminusintegratedchemicalloss,whichcanbeinterpretedastheeffectsof

transport.Red,blue,andgreencrosses:vortexaveragedozonelosscalculatedfrom1992,1993,

and1994MLSobservations,respectively.

Figure8:a.TimeseriesofAntarcticCl_y(solidlines)andCl_x(dashedlines)intheGMI_GCM

andGMI_DASsimulationsduring1995onthe450Kpotentialtemperaturesurface.$Cl_x$is

definedas$ClO+2*Cl_2O_2$.Bluelin esshowGMI_GCMresultsandredlinesshowGMI_DAS

results.Crossesareobservationally -basedestimatesofAntarcticCl_yfromCLAESN_2O

observationsasdiscussedintext.b.RatioofAntarcticCl_xtoCl_yinthetwosimulations,asa

percentageofCl_y.

Figure9:Equivalent -latitudeaveragedCl_ycomparisons.Magentaasteriskswitherrorbars

indicateCl_yinferredfromCLAESN_2OobservationsfromSeptember,1992.Blackcrossesshow

Cl_yinferredfromATLASN_2OobservationsmadeonNASAER -2flightsinOct ober,1994,as

partoftheASHOEmission.Greencrosses -Cl_yinferredfromATLASN_2Oobservationsmade

onNASAER 2flightsinSeptember,1987,aspartoftheAAOEmission.

Figure10:Comparisonofozonelossat450Kin1995,2030,andtheirdifference. a.Shows

ozonelossafterJuly1during1995inGMI_GCM(solidblueline)andGMI_DAS(solidred

line)simulations.Dashedblueandredlinesarethecorrespondinglossesfortheyear2030.

Dashed-dotlinesshow2030 -1995differenceforGMI_GCM(blue)an dGMI_DAS(red).b.

ShowschemicallyintegratedozonelossafterJuly1during1995(solidlines),2030(dashed

lines)andthe2030 -1995difference(dashed -dotlines),forGMI_GCM(blue)andGMI_DAS

(red).c.ShowsneteffectoftransportafterJuly1dur ing1995(solidlines),2030(dashedlines)

andthe2030 -1995difference(dashed -dotlines),forGMI_GCM(blue)andGMI_DAS(red).

Figure11:ChangeinAntarcticCl $_y$andCl $_x$between1995and2030at450KintheGMI_GCM

andGMI_DASsimulations.Solidblu e(red)linecorrespondsto1995 –2030changeintime

seriesofCl $_y$averagedatequivalentlatitudesabove65 ^{o}SintheGMI_GCM(GMI_DAS)

simulation.Dashedblue(red)linecorrespondsto1995 –2030changeintimeseriesofCl $_x$

averagedatequivalentlat itudesabove65 ^{o}SintheGMI_GCM(GMI_DAS)simulation.
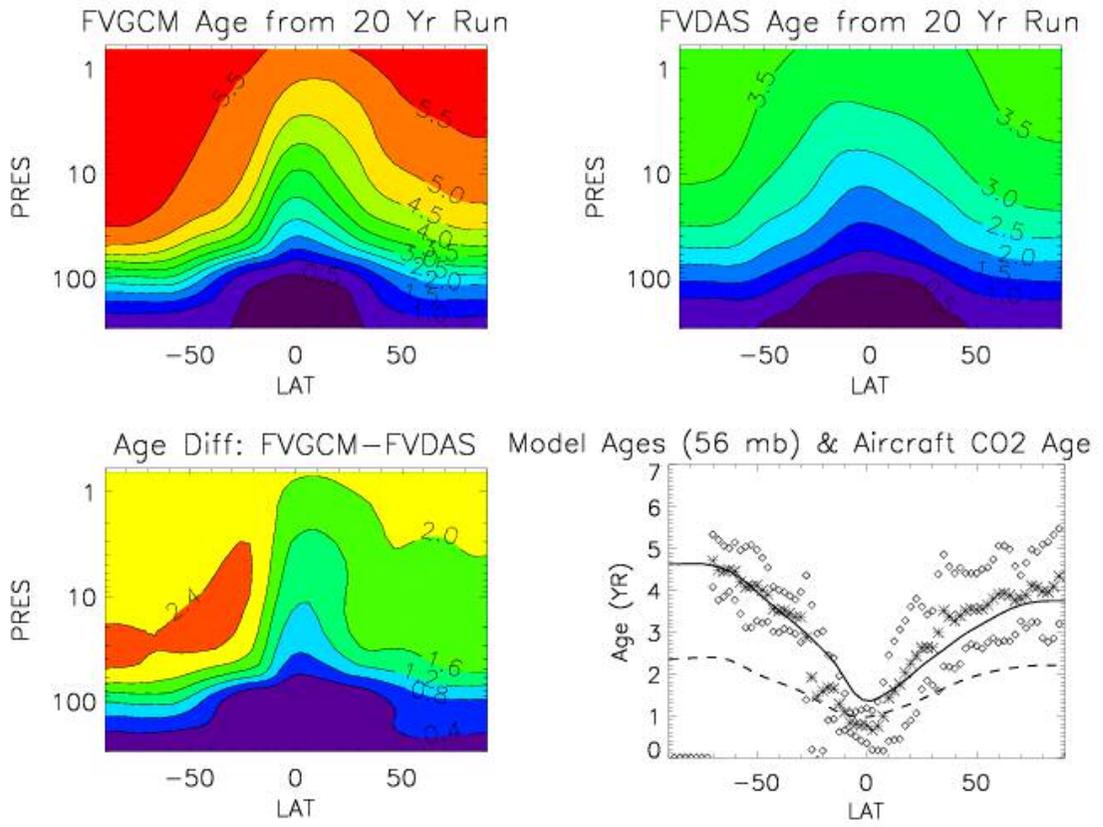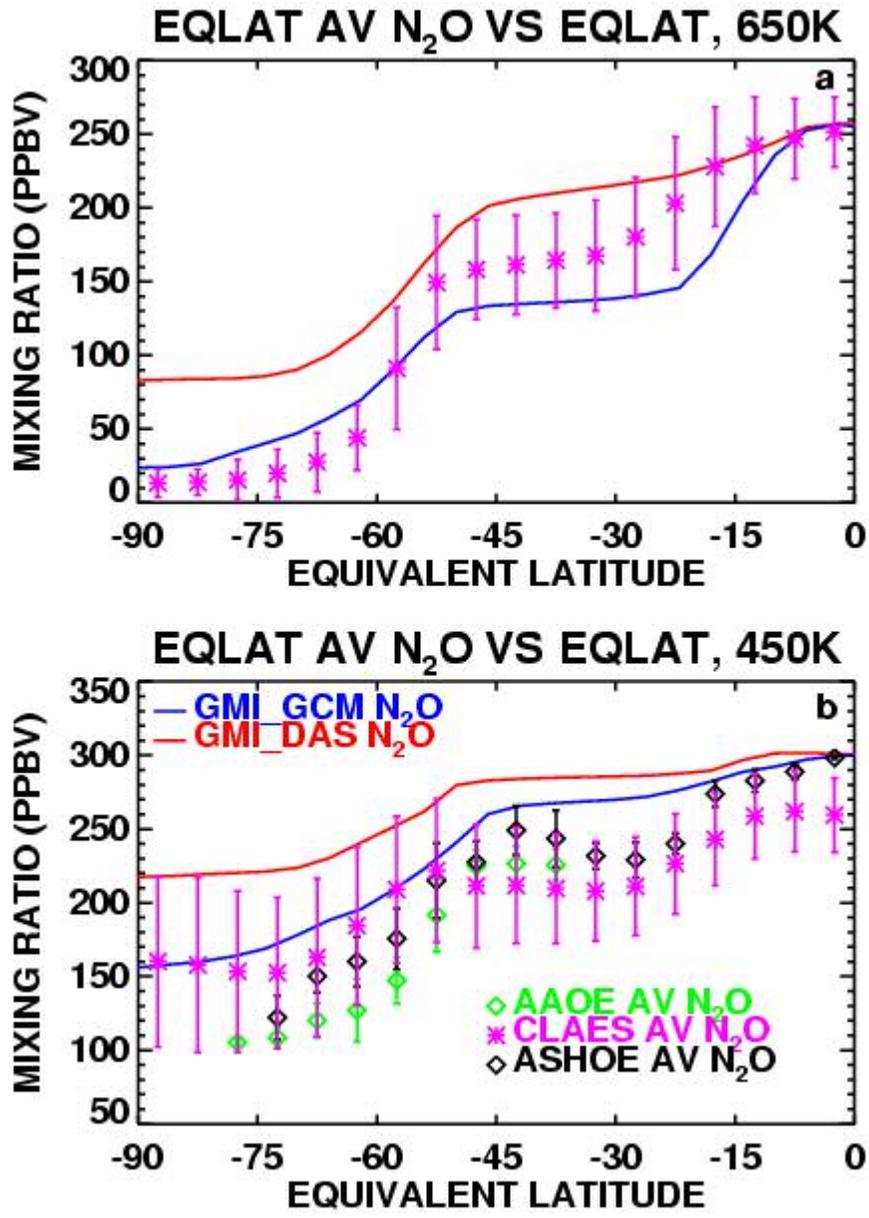
Figure1

Figure2
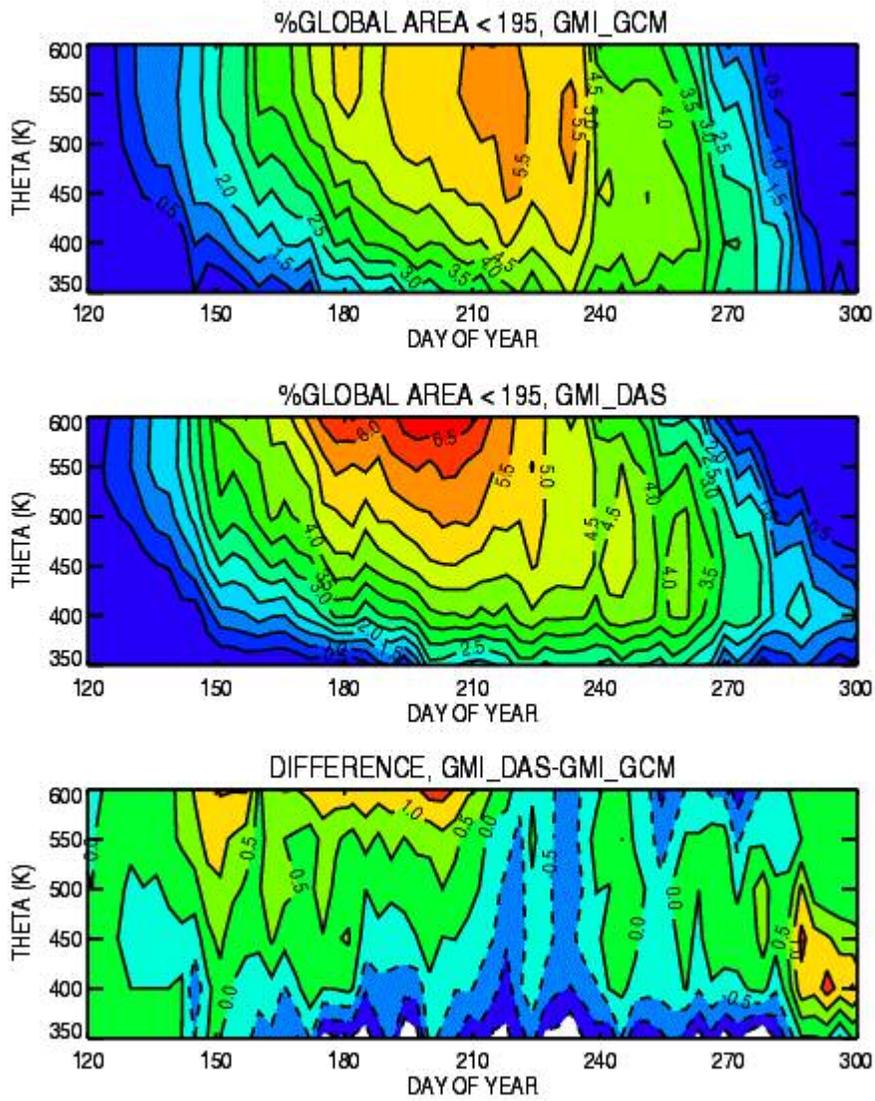
Figure3
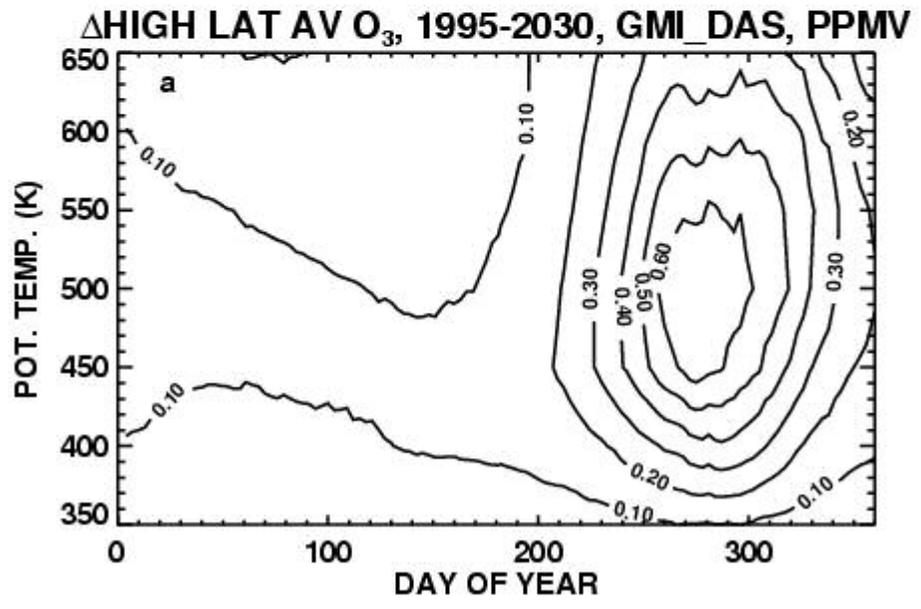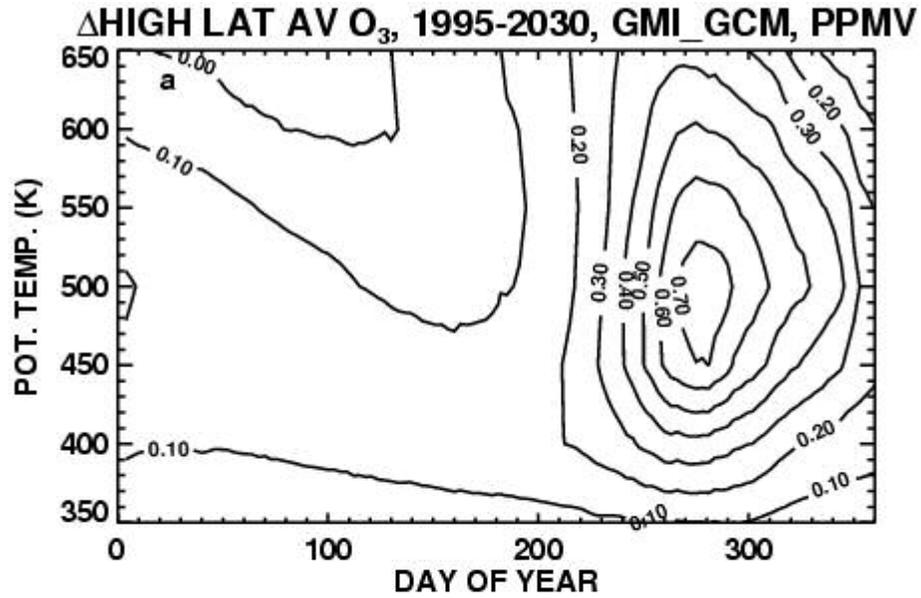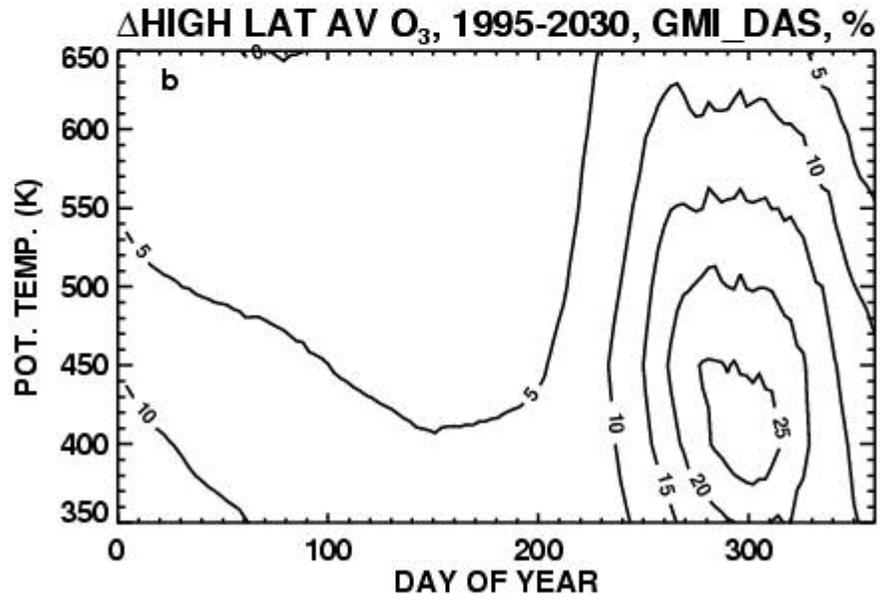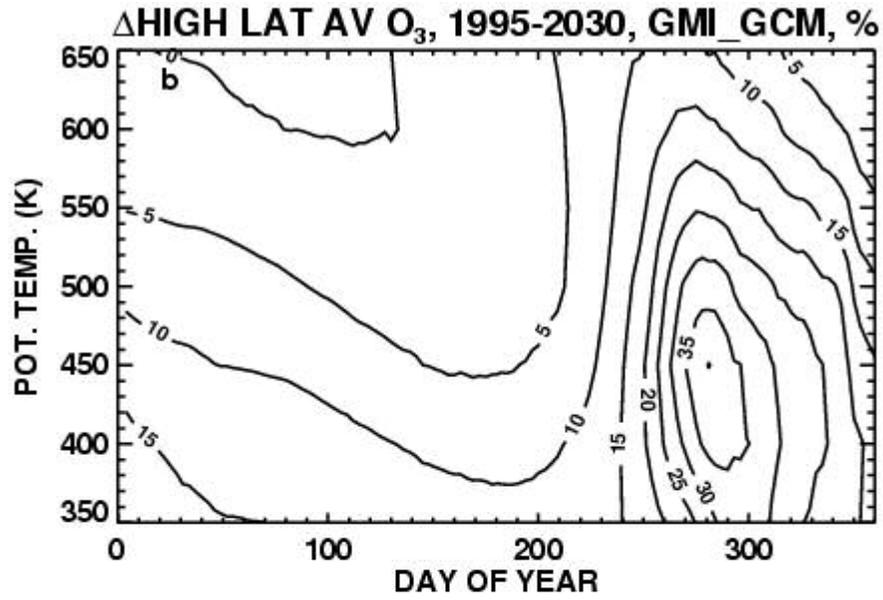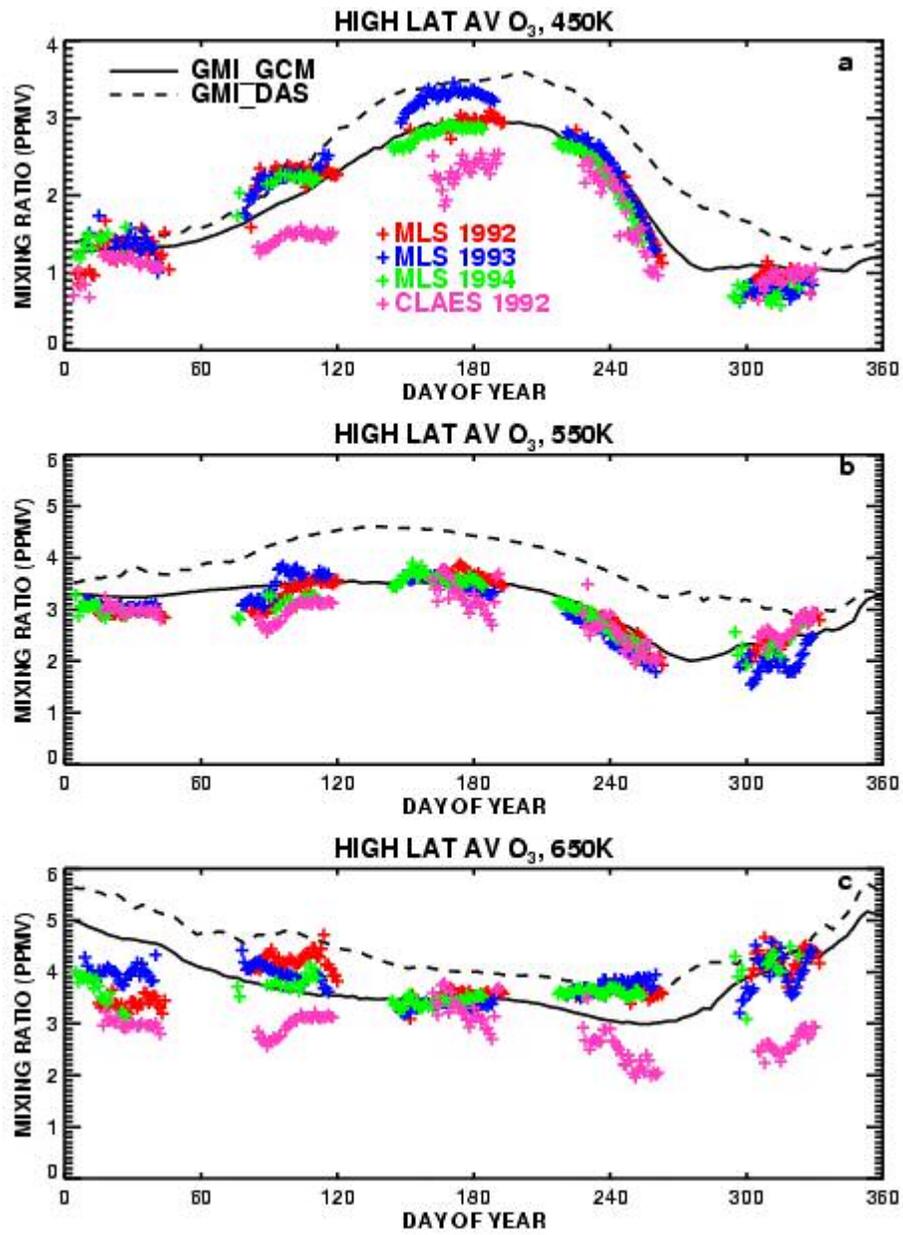
ΔHIGH LAT AV O$_3$, 1995-2030, GMI_GCM, PPMV

ΔHIGH LAT AV O$_3$, 1995-2030, GMI_DAS, PPMV

Figure4

ΔHIGH LAT AV O$_3$, 1995-2030, GMI_GCM, %

ΔHIGH LAT AV O$_3$, 1995-2030, GMI_DAS, %
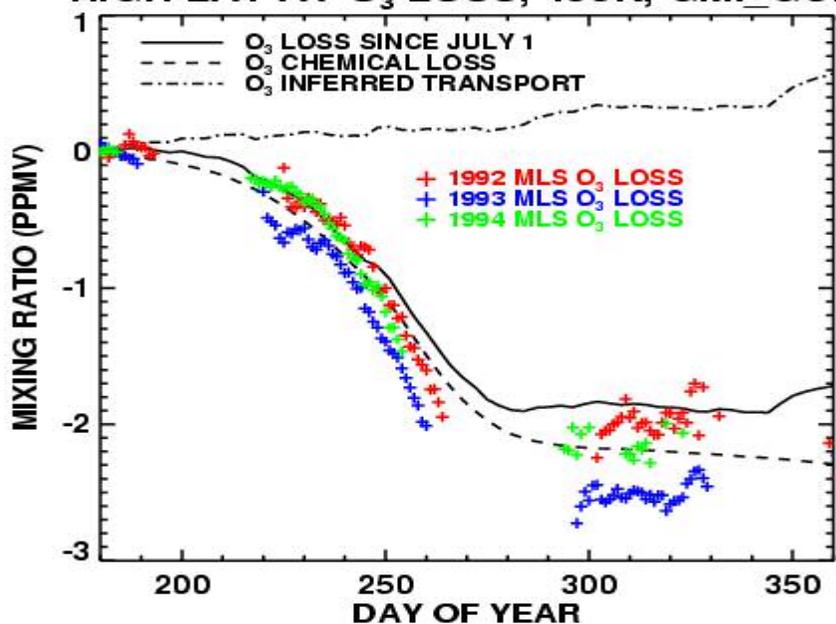
Figure5
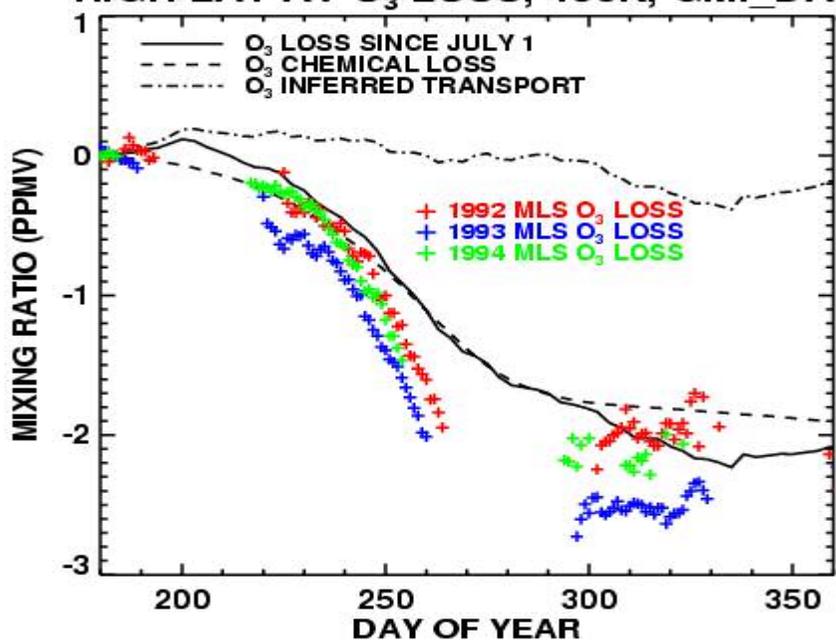
Figure6

Figure7a

Figure7b

HIGH LAT AV Cly AT 450K, 1995

— GMI_GCM Cly
— GMI_DAS Cly
+ Cly FROM CLAES N2O
- - GMI_GCM Clx
- - GMI_DAS Clx
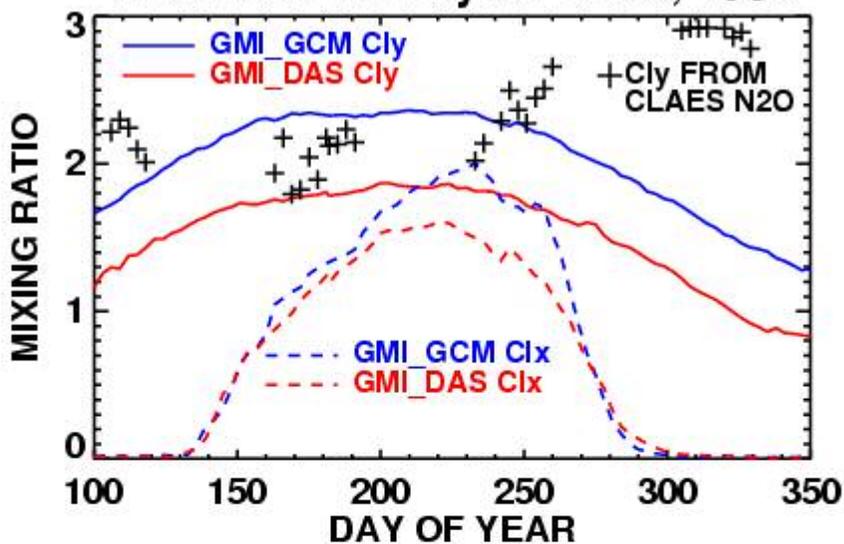
AV (ClO + 2Cl2O2)/Cly AT 450K, 1995
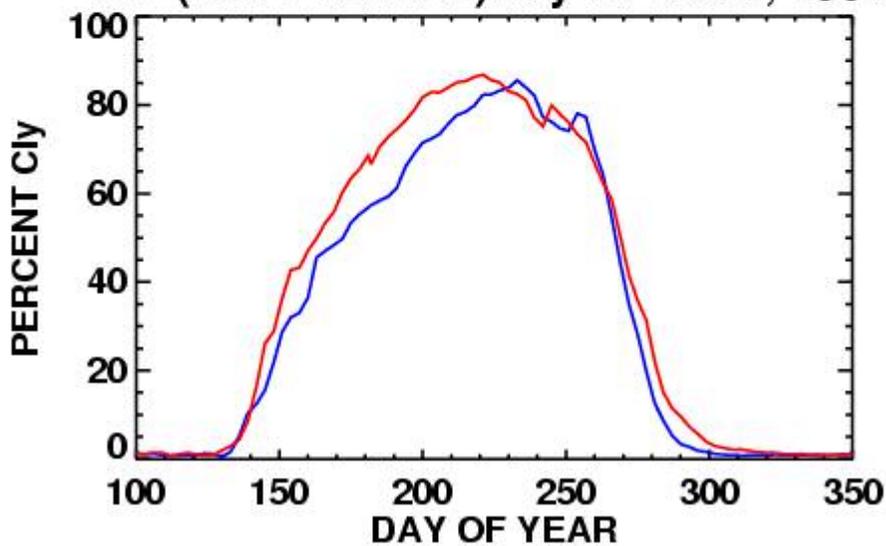
Figure8
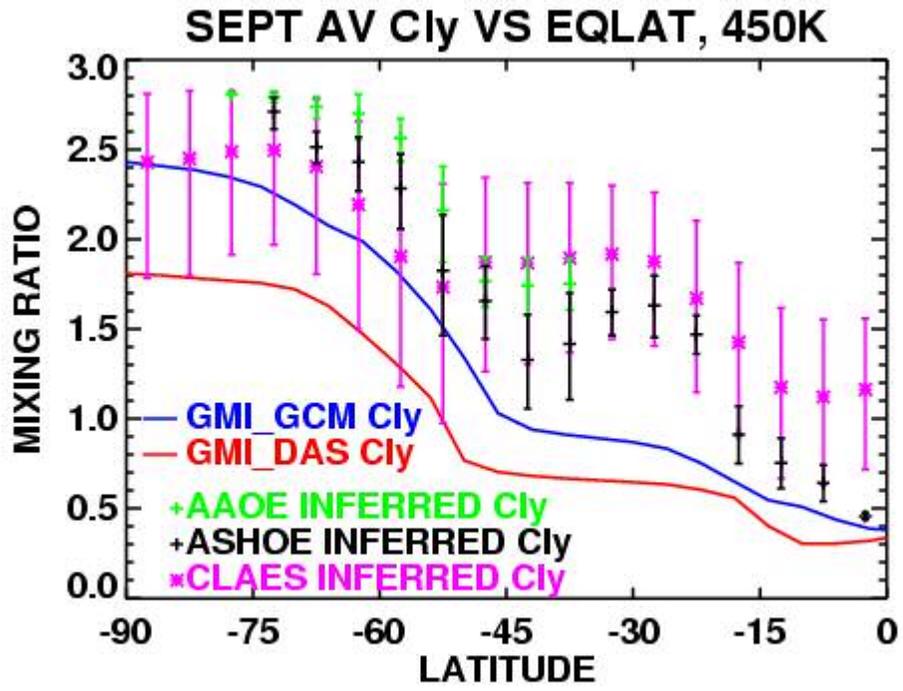
Figure9

Figure 10

Figure11